Available online at www.sciencedirect.com

SciVerse ScienceDirect

Journal of the European Ceramic Society 32 (2012) 705–710

www.elsevier.com/locate/jeurceramsoc

Fabrication of SiCN–$Sc_2Si_2O_7$ coatings on C/SiC composites at low temperatures

Jia Liu [a], Litong Zhang [a], Juan Yang [a], Laifei Cheng [a], Yiguang Wang [a,b,*]

[a] National Key Laboratory of Thermostructure Composite Materials, Northwestern Polytechnical University, Xi'an, Shaanxi 710072, PR China
[b] State Key Laboratory of Solidification Processing, Northwestern Polytechnical University, Xi'an, Shaanxi 710072, PR China

Received 30 May 2011; received in revised form 17 September 2011; accepted 30 September 2011
Available online 29 October 2011

Abstract

SiCN–$Sc_2Si_2O_7$ environmental barrier coatings were fabricated on the surface of C/SiC composites at low temperatures by adding Li_2CO_3 as sintering aids. With this addition, the fabrication temperature could be lowered about 100–200 °C. The shrinkage of the polysilazane–$Sc_2Si_2O_7$ bars with and without Li_2CO_3 was tested by dilatometer. The results indicate that the shrinkage speed of the polysilazane–$Sc_2Si_2O_7$ bar with Li_2CO_3 is faster than the one without Li_2CO_3, indicating that the Li_2CO_3 greatly promotes the sintering of polysilazane–$Sc_2Si_2O_7$. Water-vapor corrosion behavior of the SiCN–$Sc_2Si_2O_7$ coated C/SiC composites was carried out at 1250 °C. The results reveal that the SiCN–$Sc_2Si_2O_7$ coatings can effectively protect the C/SiC composites. The corrosion resistance of SiCN–$Sc_2Si_2O_7$ coatings is not degraded by adding Li_2CO_3.

Keywords: Environmental barrier coatings; $Sc_2Si_2O_7$; Sintering aid; Lithium carbonate

1. Introduction

Continuous fiber-reinforced silicon carbide matrix ceramic composites (CFCC-SiC) have been considered as promising structural materials for high temperature applications due to their excellent properties at high temperatures, such as damage tolerance, high strength, and durability.[1,2] The CFCC-SiC can be used in dry and clean oxidation environments at elevated temperatures because a protective dense silica layer will be formed on the surface of the composites.[3,4] However, in the wet environments, the formed silica layer will be deteriorated by water vapor due to the formation of volatile silica hydroxide, resulting in the mass loss and failure of the composites.[5–7] Consequently, environmental barrier coatings (EBCs) are applied on the top of CFCC-SiC components to prevent them from water vapor attack.[8–11]

Several technologies have been developed for preparation of EBCs including chemical vapor deposition (CVD),[12] plasma spray,[13] laser ablation,[14,15] sol–gel process, [16] and slurry process.[17,18] Compared with other technologies, the slurry process is able to fabricate EBCs on complex shaped components at low cost.[18] However, this technology requires very high heat-treatment temperature to obtain dense coatings. The high temperature can damage the composites to some extent.[19] For example, the properties of SiC fibers in the SiC/SiC composites are degraded at high temperatures as a result of carbothermal reduction reaction and β-SiC grains growth in the fibers.[19,20] The technology of fabricating the EBCs at low temperatures is thus highly desired.

In order to decrease the sintering temperature of ceramics, appropriate sintering aids can be added to improve the atoms diffusivity by increasing the number of crystal defects and decreasing the resistance of mass transference.[21] In this study, Li_2CO_3 was chosen as the sintering aids. In addition, liquid polysilazane was added during the preparation of the $Sc_2Si_2O_7$ slurry for the coatings. The liquid polysilazane can not only serve as a binding agent to prevent the coatings from cracking during heat-treatment, but also it can promote the densification of ceramics.[22] Moreover, the resultant ceramics from polysilazane show good oxidation resistance at high temperatures.[4,23]

In this paper, the SiCN–$Sc_2Si_2O_7$ coatings were fabricated on the 2D C/SiC composites at relatively low temperatures with

* Corresponding author at: State Key Laboratory of Solidification Processing, Northwestern Polytechnical University, Xi'an, Shaanxi 710072, PR China. Tel.: +86 29 88494914; fax: +86 29 88494620.
E-mail address: wangyiguang@nwpu.edu.cn (Y. Wang).

0955-2219/$ – see front matter © 2011 Elsevier Ltd. All rights reserved.
doi:10.1016/j.jeurceramsoc.2011.09.029

the slurry of $Sc_2Si_2O_7$, polysilazane, and Li_2CO_3. The sintering process was characterized by dilatometer. The water-vapor corrosion behavior of the coated C/SiC composites was studied at 1250 °C for 200 h. The results indicated that the addition of Li_2CO_3 did not deteriorate the corrosion resistance of $Sc_2Si_2O_7$.

2. Experimental

The liquid polysilazane (Institute of Chemistry, Chinese Academy of Science, Beijing, China) and scandium disilicate ($Sc_2Si_2O_7$) were chosen as starting materials. The viscosity of polysilazane was 12–200 cp at room temperature. The $Sc_2Si_2O_7$ powders were prepared using a sol–gel process. $Sc(NO)_3{\cdot}6H_2O$ (analytical reagent, Qing Da Fine Chemical, Yutai, China) and tetraethoxysilane (TEOS, Tianjin Bodi Chemical, Tianjin, China) were used as the raw materials in this process. $Sc(NO)_3{\cdot}6H_2O$ and TEOS were dissolved in ethanol and distilled water solution, with added HNO_3 to maintain a pH of about 3–4. The solution was stirred using a magnetic stirrer at room temperature for 12 h until the TEOS was fully hydrolyzed. The solution was then heated in an oven at 60 °C for 10 h and 120 °C for 5 h to evaporate all of the solvent, followed by heat-treatment at 1000 °C to obtain the powders. Li_2CO_3 (analytical reagent, Fuchen Chemical, Tianjin, China) was selected as the sintering additive. Two-dimensional (2D) C/SiC composites used in this study were prepared by chemical vapor infiltration (CVI). The detail fabrication process was described in Reference 24.

The 50 wt% polysilazane was dissolved in ethanol. After stirring for 30 min, the polysilazane solution was obtained. According to the weight percent of polysilazane/$Sc_2Si_2O_7$, the 70 wt% $Sc_2Si_2O_7$ powders were added into the polysilazane solution. Two weight percent Li_2CO_3 ($Li_2CO_3/Sc_2Si_2O_7$) was also added into the solution. The mixture was then ball milled in a shock-type high-energy ball-milling machine (QM-3A High Speed Vibrating Ball Mill, Nanjing T-Boat Scietech instruments & Equipment Co. Ltd., Nanjing, China) at 120 rpm for 30 min to obtain a polysilazane–$Sc_2Si_2O_7$ slurry. The slurry was uniformly brushed on the suface of 2D C/SiC composites, followed by heat-treatment in an oven at 70 °C for 5 h and 150 °C for 5 h, respectively. The polysilazane–$Sc_2Si_2O_7$ coated C/SiC samples were heat-treated at 400 °C for 1 h under argon to allow polysilazane further thermal cross-linking. The polysilazane–$Sc_2Si_2O_7$ coatings were then pyrolyzed at 900 °C for 2 h, followed by heat-treatment at 1250 °C for 2 h with the protection of argon to obtain the SiCN–$Si_2Si_2O_7$ coatings. Detail study about the evolution of the polysilazane to SiCN ceramics at high temperatures can be found elsewhere.[25] The obtained SiCN ceramics are amorphous with a pyrolysis yield of about 50%. The final content of SiCN ceramic in the coatings can be estimated to be about 15%. The coatings without Li_2CO_3 were prepared using the same process.

To study the sintering process, the mixture of polysilazane–$Sc_2Si_2O_7$ with and without Li_2CO_3 was heat-treated at 400 °C for 2 h. The obtained powders were then pressed to rectangular samples with the size of 25 mm × 4 mm × 4 mm. The thermal dilatometer (NETZSCH DIL 402 C, Selb, Germany) was used to analyze the shrinkage of the samples from room temperature to 1500 °C with a ramping rate of 1 K/min.

The water vapor corrosion behavior of $Sc_2Si_2O_7$ coated C/SiC composites was investigated in 50% H_2O–50% O_2 water vapor flow at a rate of 8.5×10^{-4} m s^{-1} (the flowing rate was estimated at room temperature) with a total pressure of 1 atm at 1250 °C. The water vapor was introduced into the alumina tube by means of oxygen carrier gas bubbling through the distilled water heated at 81.7 °C. Heating tape was used to keep the tube at a temperature of 120 °C on the water vapor entrance side of the furnace, which prevented condensation of the water vapor. The water vapor that condensed at the exit side of the tube was collected and used to verify our experimental conditions of 50% H_2O–50% O_2. The samples were put on the alumina boat crucible, and then pushed into the tube furnace. The corrosion time was up to 200 h. After corroded for 5 h, 10 h, 20 h, 50 h, 100 h, 150 h, and 200 h, the samples were taken out from the furnace and cooled to the room temperature in a desiccator quickly for weight test. At 10 h, 50 h, 100 h, and 200 h, five corroded samples with coatings were taken out for flexural strength test. As comparison, the C/SiC samples without SiCN–$Sc_2Si_2O_7$ coatings were also corroded under the same conditions.

The weight change as a function of corrosion time was measured using an electronic balance with an accuracy of 0.01 mg (Mettler Toledo AG135, Schwerzenbach, Switzerland). At least five samples were used for measurement. The average value was obtained for each point.

The flexural strength of samples was measured using a three-point bending test (Sanscmt 4304, Shenzhen, China) with a span of 30 mm. The loading rate was 0.05 mm min^{-1}. The dimension of the samples was 40 mm × 5 mm × 3.5 mm. At least five samples were used for each point on the plot.

The microstructures of the samples were observed by scanning electron microscope (JEOL-6700F, Tokyo, Japan) and the elemental analysis was conducted by energy-dispersive spectroscopy (EDS). X-ray diffraction (XRD) investigation was carried out by using a Rigaku D/max-2400 diffractometer (Tokyo, Japan) with Cu Kα radiation. Data were digitally recorded in a continuous scan in the range of angle (2θ) from 10° to 70° with a scanning rate of 0.08° s^{-1}.

3. Results and discussion

3.1. Characterization and sintering process of SiCN–$Sc_2Si_2O_7$-coated C/SiC composites

Fig. 1 shows the surface morphologies of the SiCN–$Sc_2Si_2O_7$ coatings with and without Li_2CO_3. As shown in Fig. 1a, there are a lot of pores on the surface of the SiCN–$Sc_2Si_2O_7$ coatings without Li_2CO_3. By contrast, the surface of SiCN–$Sc_2Si_2O_7$ coatings with Li_2CO_3 (Fig. 1b) is smooth without obvious cracks and pores. The enlarged morphologies of the SiCN–$Sc_2Si_2O_7$ coatings (Fig. 1c and d) indicate that the coatings without Li_2CO_3 are porous (Fig. 1c), while the ones with Li_2CO_3 are dense by the formation of liquid phase between the particles (Fig. 1d). Fig. 2 shows the cross-section of the SiCN–$Sc_2Si_2O_7$ coatings with Li_2CO_3, in which there are a few pores with

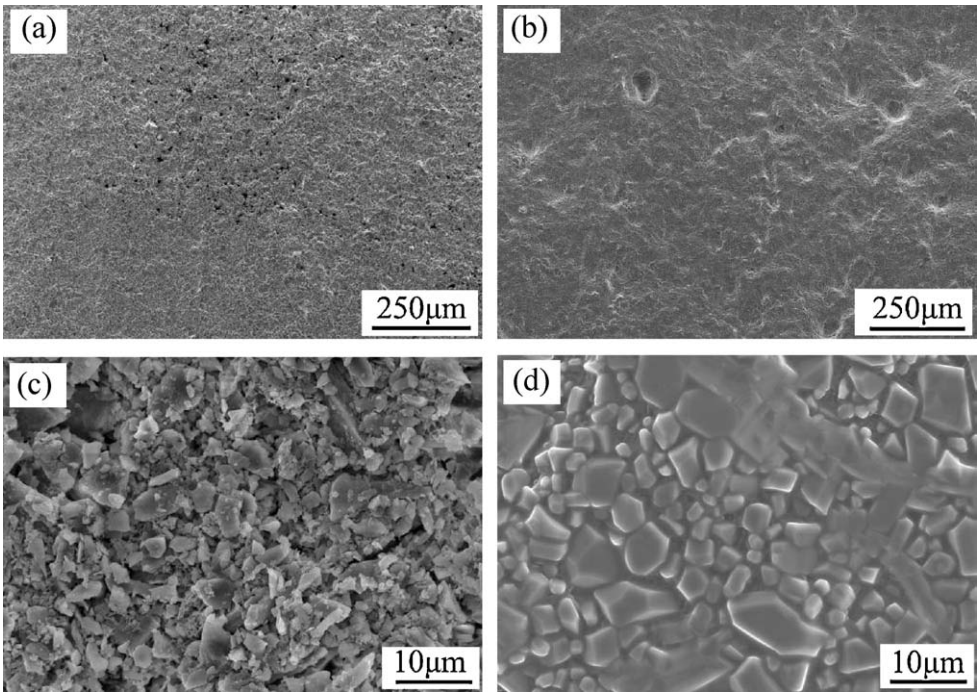

Fig. 1. Surface morphologies of SiCN–$Sc_2Si_2O_7$ coatings with and without Li_2CO_3 heat-treated at 1250 °C for 2 h under argon: (a) the surface of SiCN–$Sc_2Si_2O_7$ coatings without Li_2CO_3; (b) the surface of SiCN–$Sc_2Si_2O_7$ coatings with Li_2CO_3; (c) the enlarged morphologies of SiCN–$Sc_2Si_2O_7$ coatings without Li_2CO_3; (d) the enlarged morphologies of SiCN–$Sc_2Si_2O_7$ coatings with Li_2CO_3.

the size of micrometers. It is believed that the existing pores had resulted from the mass loss during the pyrolysis of polysilazane.[26]

When the polysilazane–$Sc_2Si_2O_7$ coatings with Li_2CO_3 are heat-treated at high temperatures, the Li_2CO_3 is decomposed to give Li_2O and CO_2. Liquid phase is formed between the particles because of the low eutectic temperature present in the Li_2O–SiO_2 system in the temperature range of 1040–1300 °C.[27,28] Mass transference through the liquid phase becomes easy. Sintering speed is thus enhanced. So the sintering process can take place at low temperatures. Fig. 3 shows the shrinkage curves (solid lines) of the polysilazane–$Sc_2Si_2O_7$ rectangular samples with and without Li_2CO_3. The differential coefficient of the shrinkage curves (dL/dt, dotted lines) expresses

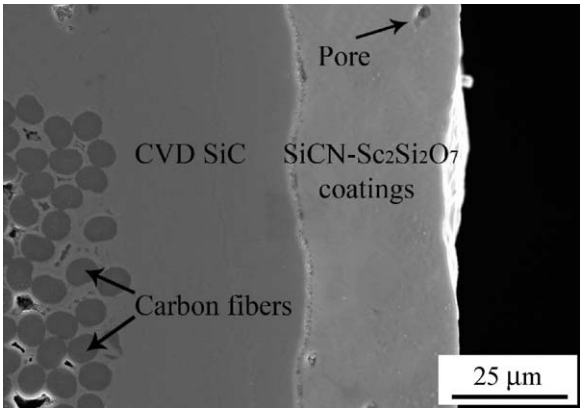

Fig. 2. Cross-section of SiCN–$Sc_2Si_2O_7$ coatings heat-treated at 1250 °C for 2 h under argon.

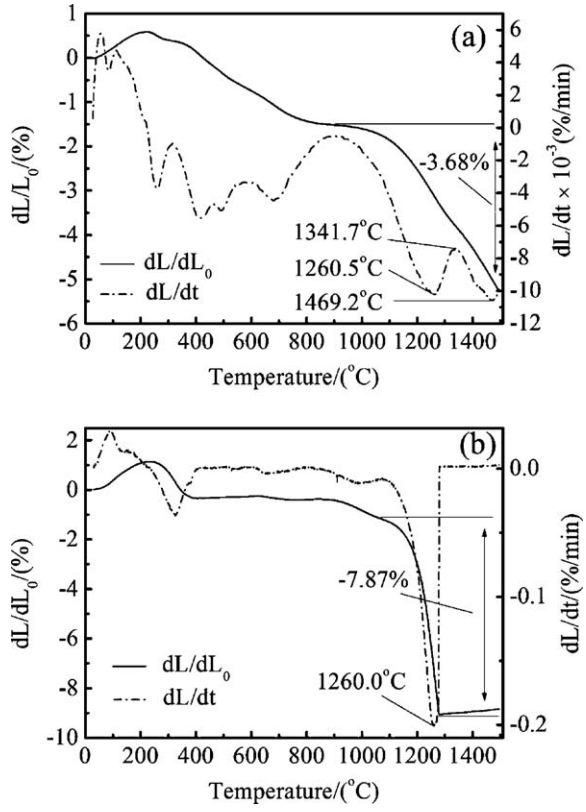

Fig. 3. Shrinkage curves of polysilazane–$Sc_2Si_2O_7$ rectangular samples with and without Li_2CO_3: (a) shrinkage curve of polysilazane–$Sc_2Si_2O_7$ rectangular sample without Li_2CO_3; (b) shrinkage curve of polysilazane–$Sc_2Si_2O_7$ rectangular sample with Li_2CO_3.

the shrinkage speed/sintering speed of the samples. As can be seen, the sintering process for the samples with/without Li_2CO_3 all begins at about 1100 °C. The shrinkage before 1000 °C is due to the pyrolysis of the polysilazane. For the sample without Li_2CO_3, the densification peak is shown at 1260.5 °C (Fig. 3a). The total shrinkage of the sample is about 3.68%. Fig. 3b shows the shrinkage curve of the rectangular sample with Li_2CO_3. The densification peak is also shown at about 1260 °C. However, the total shrinkage of the sample with Li_2CO_3 is over 7.8% (beyond the measurability), which is much higher than that of sample without Li_2CO_3. The results indicate that the sintering is enhanced by adding Li_2CO_3.

The XRD pattern of the SiCN–$Sc_2Si_2O_7$ coatings indicates that the main phases are $Sc_2Si_2O_7$, SiC, and a little of SiO_2 (Fig. 4). The signal of crystal SiC is from C/SiC matrix. The signal of SiO_2 is from the free silica in $Sc_2Si_2O_7$. There is no signal of SiCN because the SiCN is still amorphous at temperatures below 1400 °C.[25,29]

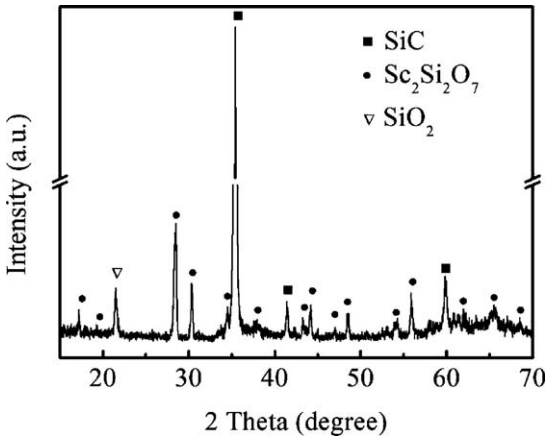

Fig. 4. XRD pattern of SiCN–$Sc_2Si_2O_7$ coating heat treated at 1250 °C for 2 h.

3.2. Water vapor corrosion behavior of the SiCN–$Sc_2Si_2O_7$ coated C/SiC composites

Water vapor corrosion behavior of the SiCN–$Sc_2Si_2O_7$ coated C/SiC composites was carried out at the temperature of 1250 °C. Fig. 5 shows the cross-sectional morphologies of C/SiC composites with and without SiCN–$Sc_2Si_2O_7$ coatings after water vapor corrosion at 1250 °C for 200 h. It can be seen that the C/SiC composites are well protected by the SiCN–$Sc_2Si_2O_7$ coatings (Fig. 5a). Carbon fiber inside are not oxidized by oxygen/water vapor even after corrosion for 200 h. There is a reaction zone between the coatings and substrate. The EDS spectrum of the reaction zone shows that the compositions in this zone are mainly silicon and oxygen, which indicates that the zone is composed of silica. It is believed that the silica layer originates from the oxidation of SiC by oxygen diffusing through the SiCN–$Sc_2Si_2O_7$ coatings.[26] The silica layer can be benefit for the oxidation resistance by preventing oxidative gas diffusion through. For the composites without SiCN–$Sc_2Si_2O_7$ coatings, CVD SiC coating is exposed to the water-vapor environment, the coating is oxidized to form lots of pores and cracks (Fig. 5b and c). These pores and cracks offer the channels for the steam/oxygen penetrating the coating to attack the SiC and C fibers inside. The carbon fibers are almost burnt out, leaving

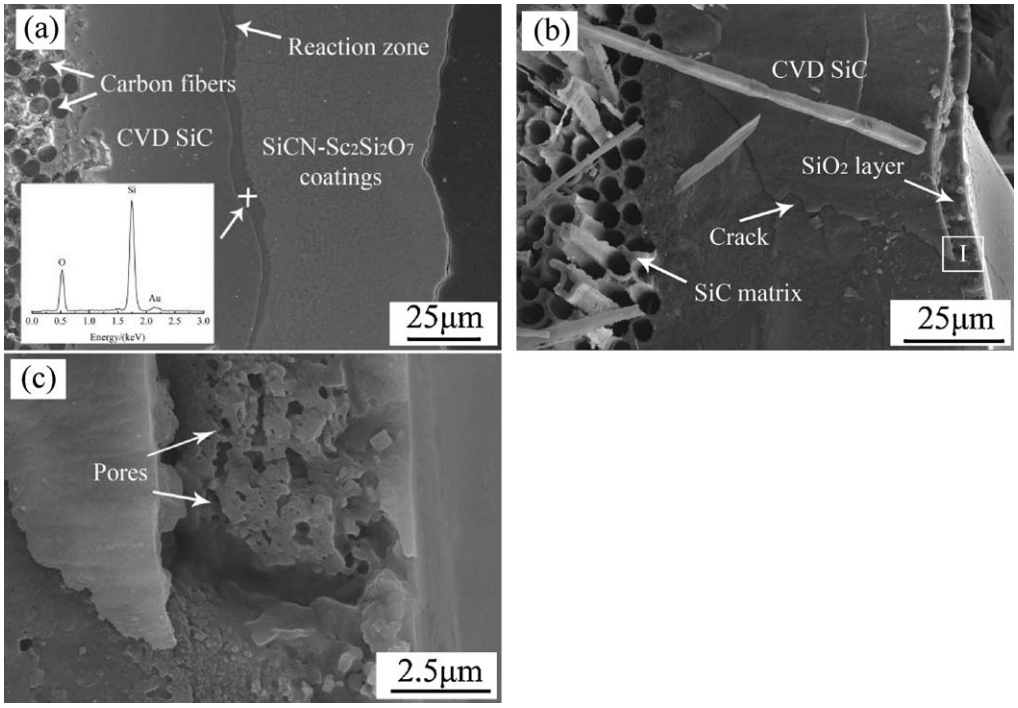

Fig. 5. The cross-sections of 2D C/SiC composites with and without SiCN–$Sc_2Si_2O_7$ coatings corroded in water vapor at 1250 °C for 200 h: (a) the composites with SiCN–$Sc_2Si_2O_7$ coatings and embedded EDS analysis of the reaction zone; (b) the composites without SiCN–$Sc_2Si_2O_7$ coatings; (c) higher magnification micrograph taken from "I" area marked in (b).

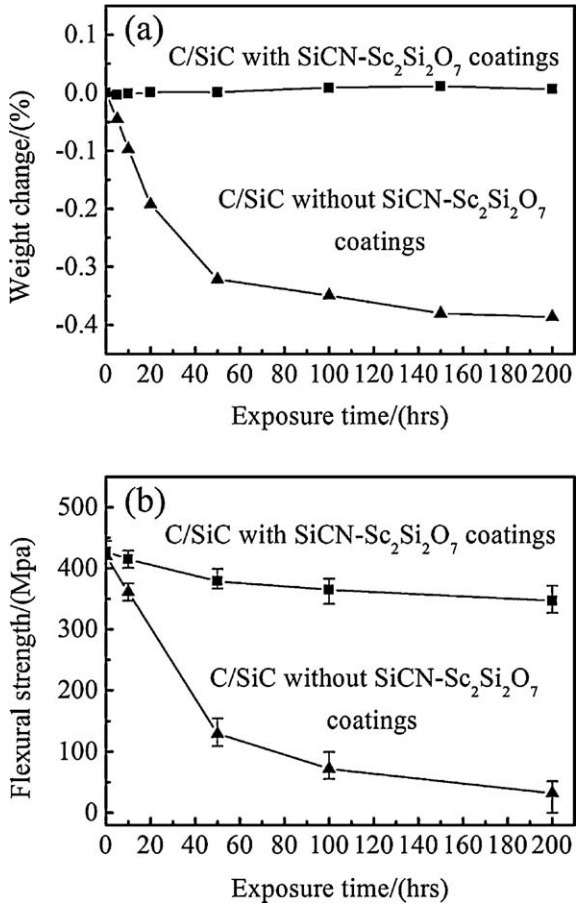

Fig. 6. Corrosion behavior of the 2D C/SiC composites with and without SiCN–$Sc_2Si_2O_7$ coatings in water vapor at 1250 °C for 200 h: (a) weight change as a function of corrosion time; (b) residual flexural strength as a function of corrosion time.

a lot of holes inside. SiC matrix and CVD SiC coating lose their protection to carbon fibers in water vapor.

Fig. 6a shows the weight loss of the C/SiC composites with and without SiCN–$Sc_2Si_2O_7$ coatings as a function of corrosion time. It is known that the water vapor will remove the silica layer, which formed by the oxidation of CVD SiC coating.[5–7] The carbon fibers will then be attacked by the oxidative gas, leading to the weight loss of C/SiC composites. However, the C/SiC composites with the SiCN–$Sc_2Si_2O_7$ coatings show little weight change in water vapor. A little weight gain can be observed after corrosion for 100 h due to the oxidation of SiC by oxygen diffusing through the SiCN–$Sc_2Si_2O_7$ coatings. The residual flexural strengths of C/SiC composites with and without SiCN–$Sc_2Si_2O_7$ coatings as a function of corrosion time are shown in Fig. 6b. The C/SiC composites with SiCN–$Sc_2Si_2O_7$ coatings can keep about 83.3% of the original flexural strength even after corroded at 1250 °C in water vapor for 200 h, while the C/SiC composites without SiCN–$Sc_2Si_2O_7$ coatings have only about 11.9% of their original flexural strength after corroded at the same conditions. The results indicate that the SiCN–$Sc_2Si_2O_7$ coatings can effectively block the water vapor attack. The corrosion resistance of the SiCN–$Sc_2Si_2O_7$ coatings is not obviously affected by adding Li_2CO_3 as a sintering additive.

4. Conclusion

The SiCN–$Sc_2Si_2O_7$ coatings were fabricated on the surface of C/SiC composites by using the liquid polysilazane and $Sc_2Si_2O_7$ as starting materials. The Li_2CO_3 was added as a sintering additive. The dense SiCN–$Sc_2Si_2O_7$ coatings were obtained after heat-treated at 1250 °C for 2 h under argon. The preparation temperature was lower 100–200 °C than that without Li_2CO_3.

Water vapor corrosion of the C/SiC composites with and without SiCN–$Sc_2Si_2O_7$ coatings were carried out at 1250 °C for 200 h. The results showed that the SiCN–$Sc_2Si_2O_7$ coatings could effectively block the water vapor attack at high temperatures, and the sintering additive did not deteriorate the corrosion resistance of the SiCN–$Sc_2Si_2O_7$ coatings. The Li_2CO_3 can be chosen as a sintering aid to lower the preparation temperature of SiCN–$Sc_2Si_2O_7$ coatings.

Acknowledgment

This work was financially supported by the Chinese Natural Science Foundation (Grant #51032006), the Research Fund of State Key Laboratory of Solidification Processing (Grant #56-TZ-2010), and partially supported by the Project "111" (B08040).

References

1. Schmidt S, Beyer S, Knabe H, Immich H, Meistring R, Gessler A. Advanced ceramic matrix composites materials for current and future propulsion technology applications. *Acta Astronsut* 2004;**55**:409–20.
2. Kaya H. The application of ceramic–matrix composites to the automotive ceramic gas turbine. *Compos Sci Technol* 1999;**59**:861–72.
3. Jacobon NS, Opila EJ, Lee KN, Oxidation. Corrosion of ceramics and ceramic matrix composites. *Curr Opin Solid State Mater Sci* 2001;**5**(4):301–9.
4. Wang YG, Fan Y, Zhang L, Zhang W, An LN. Polymer-derived SiAlCN ceramics resist oxidation at 1400 °C. *Scr Mater* 2006;**55**:295–7.
5. Jacobson NS. Corrosion of silicon-based ceramics in combustion environments. *J Am Ceram Soc* 1993;**76**(1):3–28.
6. Opila EJ. Paralinear oxidation of CVD SiC in water vapor. *J Am Ceram Soc* 1997;**80**(1):197–205.
7. Wang YG, Fei W, Fan Y, Zhang L, Zhang W, An LN. Silicoaluminum carbonitride ceramic resistance to oxidation/corrosion in water vapor. *J Mater Res* 2006;**21**(7):1625–8.
8. Lee KN. Current status of environmental barrier coatings for Si-based ceramics. *Surf Coat Technol* 2000;**133–134**:1–7.
9. Wang YG, Liu JL. Fisrt-principles investigation on the corrosion resistance of rare-earth disilicates in water vapor. *J Eur Ceram* 2009;**29**:2163–7.
10. Lee KN, Fox DS, Bansal NP. Rare earth silicate environmental barrier coatings for SiC/SiC composites and Si_3N_4 ceramics. *J Eur Ceram Soc* 2005;**25**:1705–15.
11. Wang YG, Liu JL. Water corrosion behaviors of barium aluminosilicates: a first-principles investigation. *Corros Sci* 2009;**51**:2126–9.
12. Mulpuri RP, Sarin VK. Synthesis of mullite coatings by chemical vapor deposition. *J Mater Res* 1996;**11**(6):1315–24.
13. Lee KN, Miller RA, Jacobson NS. New generation of plasma-sprayed mullite coating on silicon carbide. *J Am Ceram Soc* 1995;**78**(3):705–10.

14. Huang CM, Xu Y, Zangvil A, Kriven WM, Xiong F. Laser ablated coatings on ceramic fibers for ceramic matrix composites. *Mater Sci Eng A* 1995;**191**(1):249–56.
15. Liu QM, Zhang LT, Jiang FR, Liu J, Cheng LF, Li H, et al. Laser ablation behaviors of SiC–ZrC coated carbon/carbon composites. *Surf Coat Technol* 2011;**205**:4299–303.
16. Wang YG, Wu YH, Cheng LF, Zhang LT. Hot corrosion behavior of barium aluminosilicate-coated C/SiC composites at 900 °C. *J Am Ceram Soc* 2010;**93**(1):204–8.
17. Chen GF, Lee KN, Tewari SN. Slurry development for the deposition of a $GdSiO_4$ + mullite environmental barrier coating on silicon carbide. *J Ceram Process Res* 2007;**8**(2):142–4.
18. Ramasamy S, Tewari SN, Lee KN, Bhatt RT, Fox DS. EBC development for hot-pressed Y_2O_3/Al_2O_3 doped silicon nitride ceramics. *Mater Sci Eng A* 2010;**527**(21-22):5492–8.
19. Man T. Thermal stability of SiC fibers (Nicalon®). *J Mater Sci* 1984;**19**:1191–201.
20. Takeda M, Sakamoto J, Imai Y, Ichikawa H. Thermal stability of the low-oxygen-content silicon carbide fiber, Hi-Nicalon™. *Compos Sci Technol* 1999;**59**:813–9.
21. Yu ZB, Thompson DP, Bhatti AR. In situ growth of elongated α-sialon grains in Li-α-sialon ceramics. *J Eur Ceram Soc* 2001;**21**(13):2423–34.
22. Greil P, Seibold M. Modelling of dimensional changes during polymer–ceramic conversion for bulk component fabrication. *J Mater Sci* 1992;**27**:1053–60.
23. Wang YG, Fan Y, Zhang LG, Burton S, Gan ZH, An LN. Oxidation of polymer-derived ceramics. *J Am Ceram Soc* 2005;**88**(11):3075–80.
24. Cheng LF, Xu YD, Zhang LT, Gao R. Effect of glass sealing on the oxidation behavior of three dimensional C/SiC composites in air. *Carbon* 2001;**39**:1127–33.
25. Wang YG, Ding J, Feng W, An LN. Effect of pyrolysis temperature on the piezoresistivity of polymer-derived ceramics. *J Am Soc* 2010;**94**(2):359–62.
26. Liu J, Zhang LT, Liu QM, Cheng LF, Wang YG. Polymer-derived SiOC-BSAS coatings as an environmental barrier for C/SiC composites. *J Am Soc* 2010;**93**(12):4148–52.
27. Ota R, Mishima N, Wakasugi T, Fukunaga J. Nucleation kinetics of a $Li_2O{\cdot}SiO_2$ glass based on a liquid model. *J Mater Sci* 1999;**34**:5937–41.
28. Claus S, Kleykamp H, Smykatz-Kloss W. Phase equilibria in the Li_4SiO_4–Li_2SiO_3 region of the pseudobinary Li_2O–SiO_2 system. *J Nucl Mater* 1996;**230**:8–11.
29. Mera G, Riedel R, Poli F, Müller K. Carbon-rich SiCN ceramics derived from phenyl-containing poly(silycarbodiimides). *J Eur Ceram Soc* 2009;**29**:2873–83.